4-7 As-grown Growth of MgB_2 Thin Films and Fabrication of Josephson Junctions

SIMAKAGE Hisashi and WANG Zhen

The as-grown MgB_2 made by co-evaporation and sputtering methods were deposited at low substrate temperatures. The critical temperatures were obtained to 35 K and 29 K, respectively. The deposition was achieved at substrate temperature below 300°C, which suggested that these methods are useful for multi-layer depositions. Using the MgB_2 thin films, the MgB_2/AlN/NbN trilayer junctions were fabricated. The current voltage characteristics showed the Josephson tunneling currents and gap structures. The critical current density was over 1 kA/cm^2, and the critical current dependence on external magnetic fields showed the ideal modulation properties, which indicated the uniform Josephson currents.

Keywords
MgB_2, Co-evaporation, Sputtering, Thin film, Josephson junction

1 Introduction

In the fall of 2001, a group of researchers at Aoyama Gakuin University published a report in Nature on a new superconducting material, MgB_2 (magnesium boride), which has a critical temperature of 39 K [1], the finding of which sent shock waves around the world. The discovery of superconductivity in Hg traces back to 1911. Since then, various metals and metal compounds have been confirmed to show superconductivity. However, no improvement in the critical temperature had been reported since 23 K for Nb_3Ge. The discovery of a series of high temperature superconductors that started in the La-related materials in 1986 increased the critical temperature dramatically. It is still well remembered how superconductors with critical temperatures above the 77 K liquid nitrogen temperature raised a superconductivity fever not only in the superconductor research community but also in the general public. Compared to high temperature superconductors, MgB_2 has a low critical temperature. Nevertheless, this critical temperature is the highest among the metal compound superconductors. It is a common substance that appears in material catalogues but its superconductivity had been overlooked. While various borides are known to show superconductivity, it seems MgB_2 alone was accidentally omitted from these investigations. The group at Aoyama Gakuin University studied the appearance of superconductivity in the 3-element system of Mg, B, and Ti, and finally discovered superconductivity in the 2-element system of Mg and B, without Ti. Figure 1 shows the crystalline structure of the compound. The crystalline structure is a simple hexagonal system, and the separate Mg and B layers repeat in the c-axis direction.

The NICT are presently conducting studies on high frequency superconductivity applications. To apply the superior techniques established for superconductor detectors using conventional Nb superconductors to MgB_2, a number of problems must be solved. The first is thin film fabrication. Without high quality thin film fabrication techniques, no success

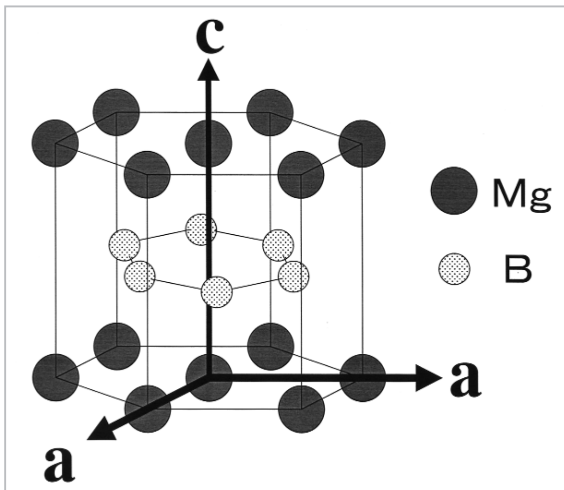

Fig.1 *Crystalline structure of MgB_2*

can be expected in developing superconductor devices. MgB_2 is a relatively stable substance, but metallic magnesium (Mg) is extremely reactive, is easily oxidized, and has a low melting point of 650°C. On the other hand, the melting point of boron (B) is as high as 2,550°C. The large difference in the characteristics of these two elements is considered to be the cause of the difficulties in fabricating a thin film of MgB_2. Several groups have attempted fabricating thin films mainly based on two-step fabrication methods, including a high temperature annealing process at approximately 800°C. These methods deposit the Mg-B or B initial film at room temperature via the laser deposition method or the electron beam evaporation method. Then, the film is processed through high temperature annealing in an Mg atmosphere at or above 600°C. These processes are reported to produce thin films with superior crystallinity and a critical temperature of approximately 39 K [2]. However, fabrication methods that involve high temperature annealing may cause problems in producing devices that require multilayer thin film structures, such as the deterioration of film quality due to re-crystallization within layers, and diffusion at the interface between layers. These problems limit the number of applications. Thus, for MgB_2 device applications, the growth of high quality as-grown MgB_2 thin films must be achieved at low temperatures. As the next step after the fabrication of the thin film, it is also desired that the SIS junctions be constructed using MgB_2. Several research institutions are conducting studies on the fabrication of the SIS junctions, but the ideal junction characteristics as observed in conventional superconductors have not yet been obtained.

According to the phase diagram of Mg-B mixtures [3], there is a region in which the gas phase of Mg and MgB_2 coexist, indicating the possibility of a relatively low temperature film synthesis condition at approximately 300°C. The present report discusses the as-grown low temperature thin film fabrication based on two methods developed at the NICT: the co-evaporation method [4], and the sputtering method [5]. It also discusses a layered Josephson junction [6] fabricated using the obtained thin film.

2 Fabrication of superconducting thin films

2-1 Co-evaporation method

Figure 2 shows the schematic diagram of MgB_2 thin film deposition based on the co-evaporation method. Mg is evaporated via resistance heating and B is evaporated by electron beams. The evaporation sources are arranged so that they do not interfere with each other. A film thickness controller maintains a steady evaporation rate for each source. The substrate is set in an inconel holder and heated to 200°C to 400°C by a SiC heater. To achieve epitaxial growth in the thin film deposition, the selection of the optimum substrate is extremely important. The crystalline structure of MgB_2 is hexagonal, and the substrate is desired to have the same hexagonal crystalline structure for epitaxial growth. The c-plane sapphire substrate is one of the substrates that has a hexagonal crystalline structure. The length of the a-axis of c-plane sapphire is 4.777 Å whereas that of MgB_2 is 3.086 Å, the mismatch being as large as 43%. However, the c-plane sapphire substrate is selected for the MgB_2 growth due to its stable material characteristics, and its low reactivity with MgB_2.

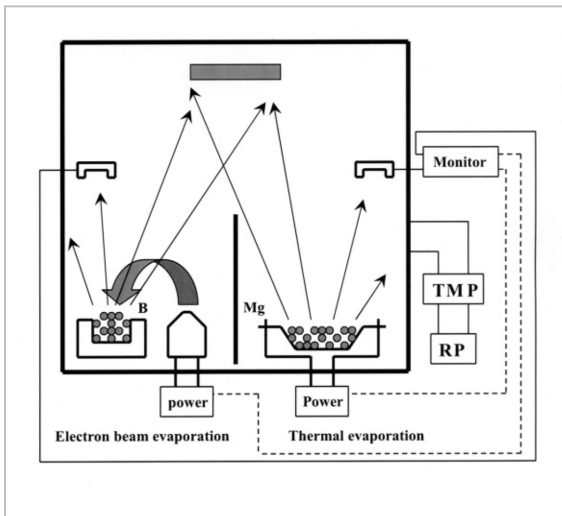

Fig.2 *Schematic diagram of MgB_2 thin film deposition equipment utilizing co-evaporation method*

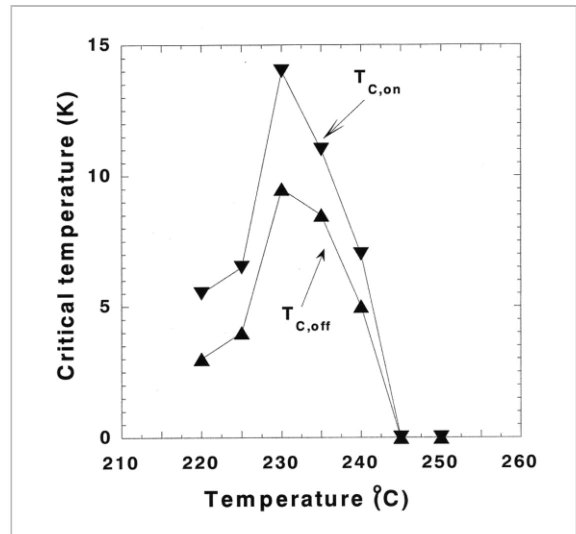

Fig.3 *Dependence of critical temperature on deposition temperature*

After setting the substrate in the deposition chamber, the vacuum chamber is pumped down to a pressure in the order of 10^{-7} Torr. As Mg is highly reactive—it readily reacts with oxygen and other substances—the high vacuum in the chamber is essential for the deposition of an MgB_2 film. Then, the substrate is heated to a predetermined temperature, and the evaporation of Mg and B is commenced. After the stability of the evaporation rates is confirmed, the shutter in front of the front face of the substrate is opened to start the deposition. After the deposition, the substrate is cooled to room temperature while maintaining the vacuum.

Figure 3 shows the dependence of the critical temperature on the substrate temperature when the evaporation rate of Mg is 5 Å per second and the evaporation rate of B is 0.5 Å per second. The upper and lower plots indicate the onset and offset of the critical temperature, respectively. The critical temperature is relatively low at less than 15 K even at the onset. However, there is a peak obtained at the substrate temperature of 230°C. It is a characteristic that the critical temperature is zero at and above 245°C. The film is almost completely insulating in this region. This behavior is considered to occur as the high vapor pressure of Mg causes re-evaporation of Mg from the substrate at 245°C, leaving insuf-

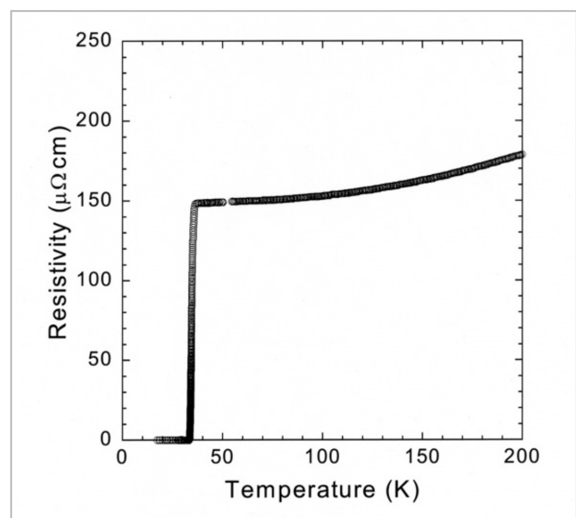

Fig.4 *Resistivity-temperature characteristics of MgB_2 thin film fabricated by co-evaporation method*

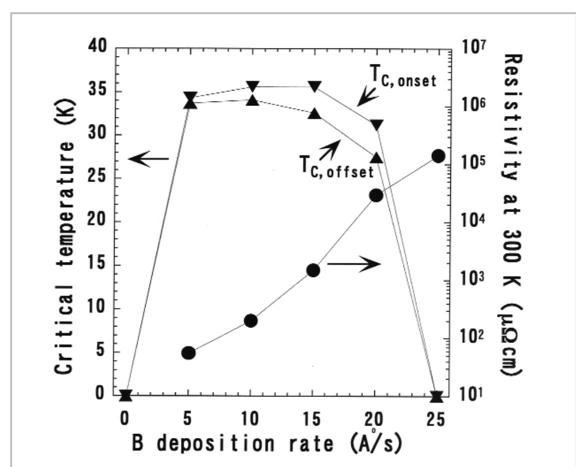

Fig.5 *Dependencies of critical temperature and resistivity on deposition rate of B*

ficient supply of Mg on the substrate for the synthesis of MgB_2, which results in the formation of a B film. A high substrate temperature is necessary to crystallize the thin film, but is concurrently disadvantageous as it prevents re-evaporation. To overcome this problem, it was believed that a higher Mg evaporation rate would promote the MgB_2 deposition at high temperatures. Figure 4 shows the resistivity-temperature characteristics of the thin film at the substrate temperature of 290°C with the evaporation rate of Mg increased to 20 Å per second and the evaporation rate for B at 10 Å per second. The critical temperature increases to approximately 35 K and the resistivity at 40 K also improves to 150 $\mu\Omega$cm. The large increase in the evaporation rate of Mg enables the deposition in the high temperature region, which was not possible at a low evaporation rate. Improvements are also confirmed in the quality of the thin film. To obtain the optimum deposition conditions, the dependence of the thin film characteristics on the evaporation rate of B is studied with the evaporation rate of Mg fixed. Figure 5 shows the results. The evaporation rate of Mg is 20 Å per second and the substrate temperature is 290°C. In the same figure, the resistivity of the fabricated thin film at 300 K is plotted versus the substrate temperature. When the evaporation rate of B is zero—in other words, when only Mg is evaporated—the Mg completely re-evaporates from the substrate and thus no film is deposited on the substrate. When the evaporation rate of B is 25 Å per second, the resistance shows a semiconductor characteristic without superconductivity. When the evaporation rate of B is between 5 Å per second and 20 Å per second, films with critical temperatures above 25 K are deposited. However, the resistivity at 300 K gradually increases as the evaporation rate of B increases. Considering that the vertical axis is logarithmic, the increase in resistivity largely depends on the evaporation rate of B. At the substrate temperature of 290°C, Mg cannot remain on the substrate in vacuum. Thus, the Mg that has reacted with B remains on the substrate as MgB_2 and the unreacted Mg is considered to re-evaporate. The increase in resistivity is considered to be dependent on the content of the unreacted B in the thin film. In other words, as B alone is a semiconductor with extremely high resistivity, the increased content of B in MgB_2 increases the resistivity of the thin film. Based on these results, it is postulated that if precise control of the deposition conditions were possible, fabrication of a stoichiometric thin film could become a reality. However, the maximum critical temperature is determined by the substrate temperature, and the critical temperature will not increase above 35 K at the present maximum substrate temperature of 290°C. To overcome this limit, a higher substrate temperature is required, which would necessitate a higher Mg evaporation rate. We are now modifying the deposition equipment with the goal of obtaining thin films of a higher quality.

2-2 Sputtering method

We have demonstrated the deposition of an MgB_2 thin film with a critical temperature of approximately 35 K based on the co-evaporation method. The sputtering method is widely used for growing various type of thin films, partly because deposition is highly controllable, being dependant on the power involved. We have also attempted MgB_2 deposition using the sputtering method. Figure 6 shows a schematic diagram of the MgB_2 deposition

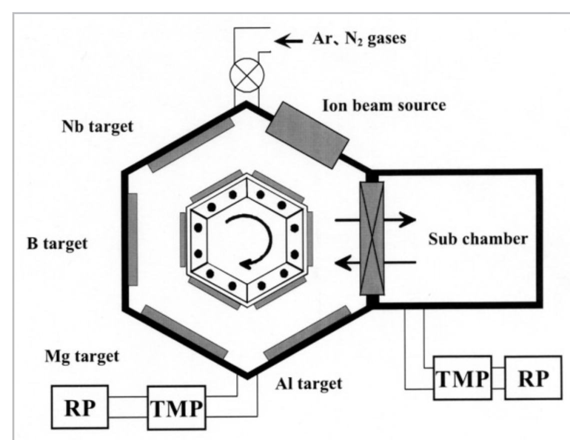

Fig.6 Schematic diagram of MgB_2 thin film deposition equipment utilizing the sputtering method

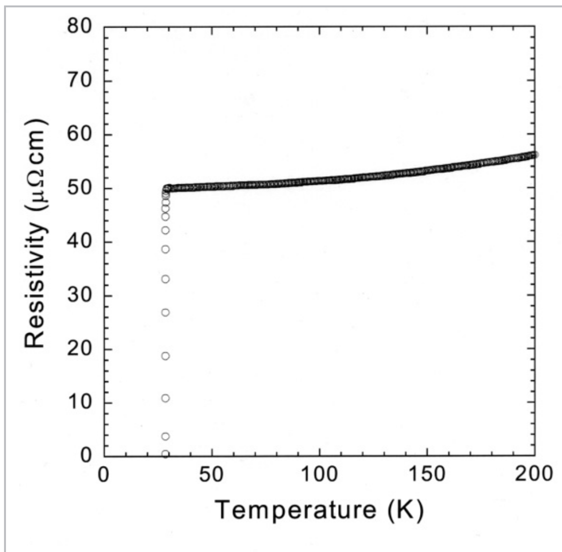

Fig.7 Resistivity-temperature dependence of MgB_2 thin film fabricated by the sputtering method

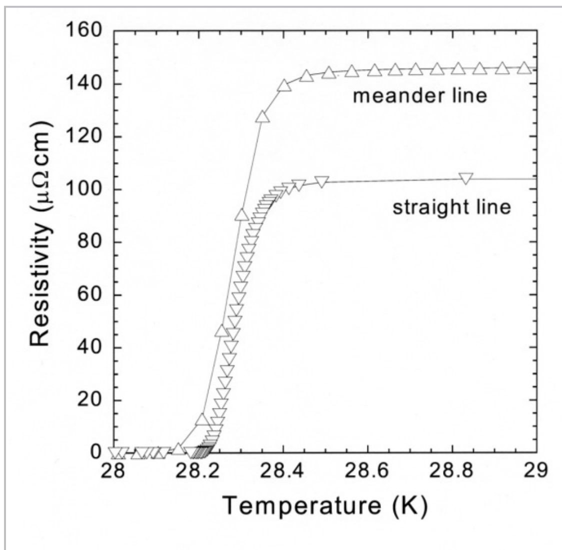

Fig.8 Resistivity-temperature dependence of 1 μm wide, 47.3 cm long meander MgB_2 thin film

equipment used in the sputtering method. The substrate holder rotates at the center, and the Mg, B, Nb, and Al single targets are arranged around the holder. To deposit an MgB_2 film, Mg and B are simultaneously sputtered at DC 300 W and AC 800 W, respectively, and the holder is rotated at 50 rpm. Nb and Al are used in the fabrication of the layered junction, discussed later. Figure 7 shows the typical resistivity-temperature characteristics of a thin film fabricated with this equipment. The critical temperature is approximately 29 K, and the resistivity at 40 K is approximately 50 μΩcm. The critical temperature is lower than that of the film fabricated by the co-evaporation method by 6 K to 7 K. In the sputtering method, it is difficult to increase the deposition rate of Mg due to the restrictions in the input power of the sputter gun and in the distance between the substrate and the targets. Although an increase in deposition rate of Mg has been shown to improve the film quality with the co-evaporation method, only a limited increase is possible in an apparatus that utilizes the sputtering method. Thus, 29 K is the limit of the critical temperature presently obtainable using this equipment. Although this critical temperature cannot be regarded as high, it realizes a low resistivity, and a low surface roughness of approximately 10 nm. To investigate the uniformity of the film, an extremely long meander of 1 μm wide and 47.3 cm long was patterned and etched on the thin film, and the temperature dependence of the resistivity was measured. Figure 8 shows the result with the resistivity of another thin film processed into a pattern 200 μm wide and 2 mm long. The critical temperature and the transition width for these two films are both approximately the same. The resistivity is also approximately the same, although a slight increase is observed for the long meander. These results demonstrate that the in-plane uniformity of the film fabricated by the sputtering method is extremely good.

3 Fabrication of Josephson junction

This section describes the fabrication of a Josephson junction that uses the MgB_2 thin film as the lower electrode. In the fabrication of the junction, the MgB_2 thin film is deposited using the sputtering method as the film uniformity is superior. Figure 9 shows the schematic diagram of the junction fabrication processes. The c-plane sapphire substrate is set on the substrate holder, heated to 290°C, and the substrate surface is cleaned using an ion beam. Then, an MgB_2 thin film of approx-

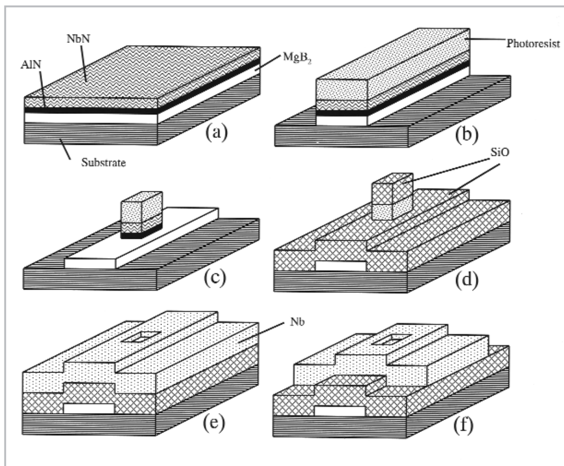

Fig.9 Fabrication processes of the MgB_2/AlN/NbN junction

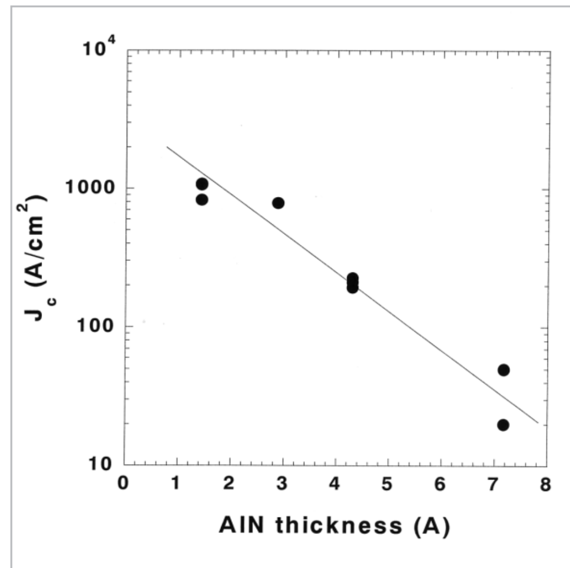

Fig.12 Dependence of critical current density on AlN film thickness

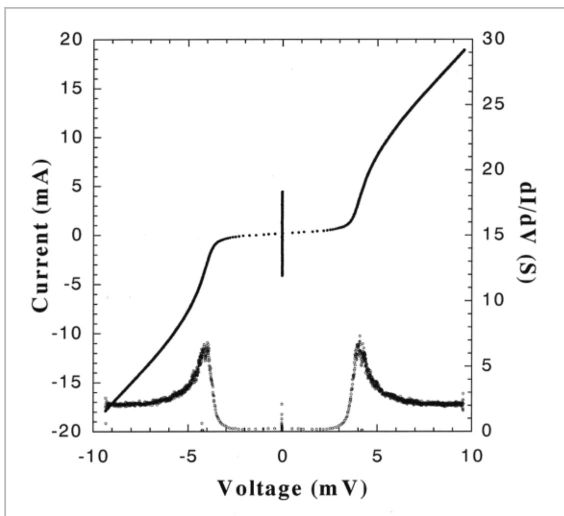

Fig.10 Current-voltage characteristics and differential characteristics of MgB_2/AlN/NbN junction

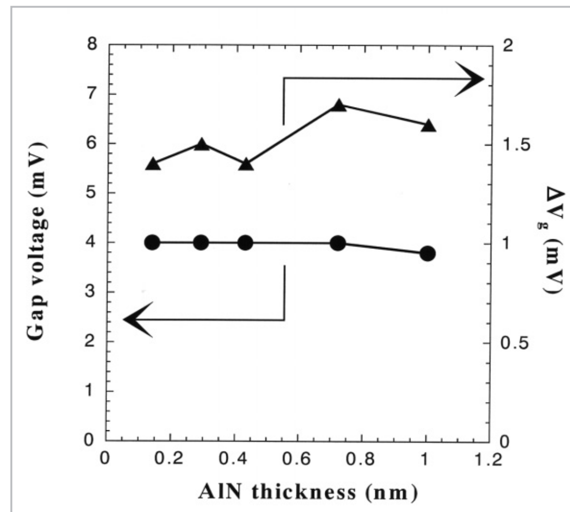

Fig.13 Dependence of gap voltage and gap voltage width on AlN film thickness

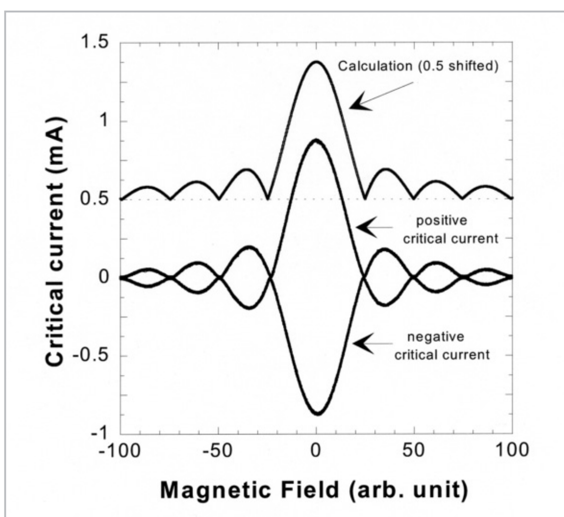

Fig.11 Modulation characteristics of Josephson current induced by external magnetic field

imately 160 nm is deposited. The sample is cooled in a vacuum to room temperature. The barrier layer AlN and 50 nm of the upper superconductive electrode NbN are deposited in the same vacuum (a). The entire surface is coated with a photoresist and the base electrode is patterned with ordinary light exposure. The three layers are etched as follows: NbN with the reactive ion etching, and AlN and MgB_2 with the ECR etching (b). The photoresist is removed with acetone, the square junction with sides of 5 μm to 20 μm is patterned, and the NbN upper electrode is

etched by reactive ion etching (c). Then, without removing the photoresist, an SiO interlayer insulating layer is vacuum deposited (d). The junction window is formed via the lift-off method. After ion beam cleaning of the upper electrode surface, the wiring Nb layer is deposited (e) and patterned, and the upper electrode is formed by reactive ion etching (f).

Figure 10 shows the typical I-V and dI/dV-V characteristics when no external magnetic field is applied at 4.2 K. The AlN film is 1.4 Å thick and the junction area is 20 × 20 μm^2. Typical SIS junction characteristics with a clear Josephson tunnel current and quasi-particle gap structure are obtained. A good junction is obtained with a critical junction current density of 1080 A/cm^2 and only a small leak current—as indicated by an R_{SG}/R_N ratio of 16.6, where R_{SG} is the sub-gap resistance and R_N is the normal resistance. Figure 11 shows the change in Josephson current when an external magnetic field is applied to the device. Here, the AlN film is 4.4 Å thick, and the junction area is 20 × 20 μm^2. The experimental results for the positive and negative Josephson currents are plotted at the bottom. The positive Josephson current theoretically calculated for a square shaped junction is plotted at the top. The calculated value is shifted up by 0.5 mA. Almost perfect agreement is confirmed between the experiment and the calculation. This result indicates that the Josephson current flows uniformly in the junction, which demonstrates the in-plane uniformity of the electrodes and the barrier thickness.

Figure 12 shows the dependence of the critical current density on the thickness of the AlN film. A typical result is obtained with the critical current decreasing exponentially as the thickness of the AlN film increases. The critical current density is over 1 kA/cm^2 when the thickness of the AlN film is 1.4 Å, indicating that a good SIS junction is successfully formed. However, the critical current density of the MgB_2/AlN/NbN film is smaller by approximately 4 orders than that obtained for the NbN/AlN/NbN junction [7]. Although the in-plane uniformity is superior, this result indicates the existence of an insulating layer in the direction perpendicular to the surface. We are presently investigating various aspects of the dependence of the thin film deposition conditions in order to understand the cause of generation of this insulating layer. Optimization is expected to produce thin films of higher quality.

The gap-voltage of the junction is estimated to be approximately 4 mV from the peak in the dI/dV-V characteristics shown in Fig. 10. This gap voltage is the sum of the gap values of the lower electrode MgB_2 and the upper electrode NbN. The critical temperature of NbN deposited on MgB_2 is 11 K. From the results of reference [7], the gap voltage at 11 K is estimated to be 1.8 mV. Thus, the gap voltage of MgB_2 itself is calculated to be 2.2 mV. According to the band calculation of MgB_2, the expected gap voltage is 7 mV for the σ band and 2 mV for the π band [8]. As the σ band has a two dimensional distribution and the π band has a three dimensional distribution, the band that contributes to the current transport in the axial direction is the π band. Our MgB_2 thin film is oriented in the direction of the c-axis and the current flows in this direction in a layered junction. Therefore, only characteristics related to the π band can be obtained. The estimated value for the gap voltage, 2.2 mV, is in good agreement with the predicted value, 2 mV of π band. To obtain a device with a larger gap voltage, a junction in the direction of the a or b axis, which requires orientation control of the thin film and fabrication of planer devices, is necessary.

Figure 13 shows the dependence of the gap voltage and the gap voltage width on the thickness of the AlN film. Here, the gap voltage is given by the peak of the dI/dV curve and the gap voltage width is the voltage width of this peak in the gradient. The gap voltage shows little variation when the thickness of the AlN film is changed. This result indicates that the deposition time for the AlN film does not deteriorate the superconductivity to the

extent that the gap voltage is changed. The gap voltage width does not show large variation either, though the value itself is approximately 1.5 mV, which is relatively large. Although the in-plane distribution of the superconductivity both in the lower and upper electrodes makes the gap larger, considering that the critical temperature of NbN in this device is 11 K, which is lower than the critical temperature of the bulk, 15 K, the gap width is expected to be mainly due to the contribution from the upper electrode. To evaluate the MgB_2 lower electrode precisely, we are now considering replacing the upper electrode with other superconductors and also fabricating SIN junctions.

4 Conclusion

As-grown MgB_2 superconductor thin films were synthesized at low temperatures using the co-evaporation and sputtering methods. The critical temperature is 35 K and 29 K for films prepared by the sputtering method and the co-evaporation method, respectively. These results demonstrate the utility of both methods in MgB_2 growth. A Josephson junction consisting of an MgB_2/AlN/NbN layered structure was also fabricated using the thin film obtained. The junction clearly shows a Josephson current and a gap structure. The critical current density is over 1 kA/cm^2, and the external magnetic field modulation characteristics obtained indicate superior uniformity in the tunnel current. Our thin film was deposited at low temperatures, offering various advantages for the layered structures. These advantages are utilized in the successful fabrication of the Josephson junction. Other examples of SIS junction fabrication using thin films are reported elsewhere, but without the simultaneous observation of a clear Josephson current and gap structure. Based on these achievements, we are conducting further studies with an eye forward the fabrication of an entire MgB_2 SIS junction, which uses MgB_2 in the upper electrode as well. The fabrication of a thin film type SIS junction is expected to provide a gap voltage of the superconductivity level, and information regarding the surface states. We will further develop our achievements to date and continue our research into achieving an application of MgB_2 for future core superconductivity electronic devices.

References

1 J. Nagamatsu, N. Nakagawa, T. Muranaka, Y. Zenitani, and J. Akimitsu, Nature, 410, 63, 2001.

2 W. N. Kang, H. J. Kim, E. M. Choi, C. U. Jung, and S. I. Lee, Science, 292,1521, 2001.

3 Z. K. Liu, D. G. Schlom, Q. Li, and X. X. Xi, Appl. Phys. Lett., 78, 3678, 2001.

4 H. Shimakage, A. Saito, A. Kawakami, and Z. Wang, IEEE Trans. Appl. Supercond., 13, 3309, 2003.

5 A. Saito, A. Kawakami, H. Shimakage, and Z. Wang, Jpn. J. Appl. Phys., 41, L127, 2002.

6 A. Saito, A. Kawakami, H. Shimakage, H. Terai, and Z. Wang, J. Appl. Phys., 92, 7369, 2002.

7 Z. Wang, H. Terai, A. Kawakami, and Y. Uzawa, Appl. Phys. Lett., 75, 701, 1999.

8 A. Y. Liu, I. I. Mazin, and J. Kortus, Phys. Rev. Lett., 87, 087005, 2001.

SHIMAKAGE Hisashi

Senior Researcher, Superconductive Electronics Group, Kansai Advanced Research Center, Basic and Advanced Research Department

Superconductive Electronics

WANG Zhen, *Dr.Eng.*

Group Leader, Superconductive Electronics Group, Kansai Advanced Research Center, Basic and Advanced Research Department

Superconductive Electronics